

# Effects of Secular Interactions in Extrasolar Planetary Systems

Fred C. Adams<sup>1,2</sup> and Gregory Laughlin<sup>3</sup>

<sup>1</sup>*Michigan Center for Theoretical Physics*

*Physics Department, University of Michigan, Ann Arbor, MI 48109*

<sup>2</sup>*Astronomy Department, University of Michigan, Ann Arbor, MI 48109*

<sup>3</sup>*Lick Observatory, University of California, Santa Cruz, CA 95064*

## ABSTRACT

This paper studies the effects of dynamical interactions among the planets in observed extrasolar planetary systems, including hypothetical additional bodies, with a focus on secular perturbations. These interactions cause the eccentricities of the planets to explore a distribution of values over time scales that are long compared to observational time baselines, but short compared to the age of the systems. The same formalism determines the eccentricity forcing of hypothetical test bodies (terrestrial planets) in these systems and we find which systems allow for potentially habitable planets. Such planets would be driven to nonzero orbital eccentricity and we derive the distribution of stellar flux experienced by the planets over the course of their orbits. The general relativistic corrections to secular interaction theory are included in the analysis and such effects are important in systems with close planets ( $\sim 4$  day orbits). Some extrasolar planetary systems (e.g., Upsilon Andromedae) can be used as a test of general relativity, whereas in other systems, general relativity can be used to constrain the system parameters (e.g.,  $\sin i \gtrsim 0.93$  for HD160691). For the case of hot Jupiters, we discuss how the absence of observed eccentricity implies the absence of companion planets.

*Subject headings:* Stars: Planetary systems

## 1. Introduction

The number of discovered planets in other systems is rapidly growing and the observational sample shows an astonishing diversity of architectures (beginning with Mayor & Queloz 1995; Marcy & Butler 1996). One way to characterize these planetary systems is in terms of their orbital elements, where the semi-major axis  $a$  and orbital eccentricity  $e$  are most often used. These variables are equivalent to specifying the energy and angular momentum of the orbit. Previous expectations, informed by the structure of our Solar System, predicted planetary orbits with larger values of  $a$  and smaller values of  $e$  than those found in the current observational sample. A major theoretical effort is now being put forth to provide an explanation of the observed distributions of

orbital elements, e.g., the  $a - e$  plane. In multiple planet systems, however, it can be important to keep in mind that the orbital eccentricities can vary dramatically through secular interactions on time scales that are long compared to observational baselines but short compared to the system ages. Instead of being described by a single value of eccentricity, the orbits of planets in multiple planet systems should generally be characterized by a complete distribution of eccentricity values (see also Takeda & Rasio 2005).

Secular interactions, and the apparent lack of evidence for such interactions, can be used to place constraints on observed planetary systems. For the known multiple planet systems, secular interactions place strong constraints on the possibility of additional as-yet undetected terrestrial planets. For putative single planet systems with zero or low eccentricity, the inferred absence of secular interactions (which tend to prevent small eccentricity values  $e \sim 0$ ) implies that any additional planets in the system must have small masses, small eccentricities, and/or large semi-major axes; we quantify these constraints for observed systems. For multiple planet systems with hot Jupiters (close planetary companions, e.g., in 4 day orbits), secular perturbations tend to increase the eccentricity of the inner planet, which also experiences tidal stressing forces from the star. This interplay leads to continual energy dissipation in the planet.

This paper follows a large body of previous work. Secular interactions have been studied for centuries, primarily in the context of our Solar System (Brower & van Woerkom 1950; Laskar 1988; and many others). With the discovery of extrasolar multiple planet systems (starting with Upsilon Andromedae; Butler et al. 1999), secular perturbation theory can be applied to an ever growing collection of planetary systems (e.g., Wu & Goldreich 2002). General schemes for studying secular interactions have been developed (Mardling & Lin 2002) and used to study close (hypothetical) terrestrial planets (Mardling & Lin 2004). For hierarchical planetary systems, a higher order (octopole) approximation scheme has been developed and applied to HD168443 and HD12661 (Lee & Peale 2003) and to triple star systems (Ford et al. 2000ab); an alternate approximation scheme has been developed and applied to the Upsilon Andromedae planetary system (Michtchenko & Malhotra 2004). The effects of disk potentials, and the disappearance of the disk, have been studied (Nagasawa et al. 2003) with the goal of explaining observed orbital eccentricities (see also Lubow & Ogilvie 2001). The effects of the Kozai mechanism have been explored for systems containing a binary companion (Takeda & Rasio 2005).

This paper builds upon the studies outlined above with the modest goal of using secular interaction theory to extract additional information from extant multiple planet systems. The basic theory is outlined in §2, which includes the leading order corrections for general relativity (GR). The results and applications are then presented in §3. In §3.1, we determine the distributions of eccentricity sampled by extrasolar planets over the course of their secular cycles, determine the secular time scales, and study the signature of secular eccentricity variations in the  $a - e$  diagram. We place constraints on the possibility of additional terrestrial planets residing in currently detected extrasolar planetary systems (§3.2) and place constraints on possible additional giant planets in observed hot Jupiter systems (§3.4). We explore the effects of general relativity in secular interac-

tions and show that some systems can be used to test relativity, while in other systems relativity can be used to place constraints on system parameters (§3.3). We conclude, in §4, with a discussion and summary of results.

## 2. Basic Theory of Secular Interactions

In this section we outline the basic theory of secular interactions as applied to the planetary systems of interest. Since this topic has been well studied over the past 250 years, the review is brief, and the results are presented for the purpose of further development in later sections.

To the second order in eccentricity and inclination angle, the equations of motion for eccentricity  $e_j$  and argument of periastron  $\varpi_j$  decouple from those of inclination angle and the ascending node. Following standard convention (Murray & Dermott 1999; hereafter MD99), we work in terms of the variables defined by

$$h_j \equiv e_j \sin \varpi_j \quad \text{and} \quad k_j \equiv e_j \cos \varpi_j, \quad (1)$$

where the subscript  $j$  refers to the  $j$ th planet in an  $N$  planet system. The basic equations of motion for the theory can then be written in the form

$$\frac{dh_j}{dt} = \frac{1}{n_j a_j^2} \frac{\partial \mathcal{R}_j}{\partial k_j} \quad \text{and} \quad \frac{dk_j}{dt} = -\frac{1}{n_j a_j^2} \frac{\partial \mathcal{R}_j}{\partial h_j}, \quad (2)$$

where  $\mathcal{R}_j$  the secular part of the disturbing function (see below and MD99 for further detail),  $n_j$  is the mean motion of the  $j$ th planet and  $a_j$  is its corresponding semi-major axis. To consistent order in this approximation, the relevant terms in the disturbing function take the form

$$\mathcal{R}_j = n_j a_j^2 \left[ \frac{1}{2} A_{jj} e_j^2 + \sum_{k \neq j} A_{jk} e_j e_k \cos(\varpi_j - \varpi_k) \right]. \quad (3)$$

The physics of these interactions is thus encapsulated in the  $N \times N$  matrix  $A_{ij}$ , where the number  $N$  of planets in the system is usually  $N = 2$  or  $3$  for the systems observed to date. The matrix elements can be written in the form

$$A_{jj} = n_j \left[ \frac{1}{4} \sum_{k \neq j} \frac{m_k}{M_* + m_j} \alpha_{jk} \bar{\alpha}_{jk} b_{3/2}^{(1)}(\alpha_{jk}) + 3 \frac{GM_*}{c^2 a_j} \right], \quad (4)$$

and

$$A_{jk} = -n_j \frac{1}{4} \frac{m_k}{M_* + m_j} \alpha_{jk} \bar{\alpha}_{jk} b_{3/2}^{(2)}(\alpha_{jk}). \quad (5)$$

In the diagonal matrix elements (eq. [4]), we have included the leading order correction for general relativity ( $c$  is the speed of light). Although these terms are small,  $\mu \equiv GM_*/(c^2 a_j) \ll 1$ , such small corrections to the eigenfrequencies can be important, especially when the system is near resonance. The quantities  $\alpha_{jk}$  are defined such that  $\alpha_{jk} = a_j/a_k$  ( $a_k/a_j$ ) if  $a_j < a_k$  ( $a_k < a_j$ ). The

complementary quantities  $\bar{\alpha}_{jk}$  are defined so that  $\bar{\alpha}_{jk} = a_j/a_k = \alpha_{jk}$  if  $a_j < a_k$ , but  $\bar{\alpha}_{jk} = 1$  for  $a_k < a_j$ . Finally, the quantities  $b_{3/2}^{(1)}(\alpha_{jk})$  and  $b_{3/2}^{(2)}(\alpha_{jk})$  are Laplace coefficients (MD99).

With the above definitions, the resulting solution takes the form

$$h_j = \sum_i \Lambda_{ji} \sin(\lambda_i t + \beta_i), \quad k_j = \sum_i \Lambda_{ji} \cos(\lambda_i t + \beta_i), \quad (6)$$

where the  $\lambda_i$  are eigenvalues of the matrix  $A_{ij}$  and the  $\Lambda_{ji}$  are the corresponding eigenvectors. The phases  $\beta_i$  and the normalization of the eigenvectors are determined by the initial conditions, i.e., the values of eccentricity  $e_j$  and argument of periastron  $\varpi_j$  for each planet at  $t = 0$ .

### 3. Applications to Extrasolar Planetary Systems

In this section we use the formal development reviewed above to study observed extrasolar planetary systems. First, we use the theory of secular interactions to show the relationship between the observed values of eccentricity and the underlying distribution of eccentricities that characterize the systems (§3.1). Next we use interactions, and their absence, to place new constraints on observed multiple planet systems. We can find constraints on the possible existence of additional small (terrestrial) planets in these systems by requiring that any such planets must reside far from a secular resonance (§3.2). For a particular subset of systems, we can find constraints on the viewing angle of the system, again by requiring that the systems are far from resonance (§3.3); in this latter application, the effects of general relativity are important and we elucidate the possible GR signatures in other planetary systems. In particular, some systems can be used as a test of general relativity. Finally, we can place constraints on observed systems with hot Jupiters and low (or zero) eccentricities, as typically found for such systems. In order for the eccentricities to stay low, any additional planets must be sufficiently distant (§3.4).

#### 3.1. Eccentricity Distributions and Secular Time Scales

As an application of secular interaction theory, we use the formalism described above (see MD99 for further detail) to calculate the variations in eccentricity in a sub-sample of observed extrasolar planetary systems. First, the eigenvalues  $\lambda_j$  for the multiple planet systems were calculated and converted into time scales for a collection of 19 observed multiple planet systems<sup>1</sup>. The results are listed in Table 1. Most of these multiple planet systems have secular interaction time scales in the range  $10^3 - 10^5$  yr. These time scales are much longer than any possible observational baseline (tens of years), but much shorter than the system lifetimes (which are typically several Gyr). The

---

<sup>1</sup>The orbital elements for these planets, along with predicted transit ephemerides and other information are tabulated at [www.transitsearch.org](http://www.transitsearch.org)

shortest secular time scale occurs for the GJ 876 system. Although the dynamics of this system are dominated by the 2:1 resonance between planets “c” and “b”, the secular interaction time  $\tau_3 = 4.4$  yr gives an excellent estimate of the time scale for dynamical interaction in the system. Indeed, radial velocity fits to the system must take into account the planet-planet interactions in order to obtain an acceptable fit (see, e.g., Rivera et al. 2005 and the references within).

These secular interaction times are thus long enough that observations can determine the eccentricity (and longitude of periastron) with high accuracy at the present epoch. Over much longer time scales that are not observationally accessible, however, the eccentricity (and longitude of periastron) will vary according to the appropriate secular cycles. As a result, attempts to explain the observed  $a - e$  plane must take the possibility of secular variations into account.

The net effect of secular interactions on our observational interpretation of these systems is that the measured eccentricity values are a particular sampling of an underlying distribution. Within the context of leading order secular theory, the distribution of eccentricity is determined by the formalism of §2. For each of the observed multiple planet systems considered in this paper, we have calculated the expected time variations of eccentricity and longitude of periastron according to secular theory. From this time series, we have extracted the mean eccentricity  $\langle e \rangle$ , the variance  $\sigma_e$  of the distribution, the minimum eccentricity value  $e_{min}$ , and the maximum value  $e_{max}$ . The results are listed in Tables 2 and 3 along with the (currently) observed values of eccentricity. The difference between the observed values and the mean eccentricities averaged over many secular cycles can be substantial (more than a factor of two). The width of the distribution can also be significant. For the second planet of the HD160691 system, for example, the first two moments of the eccentricity distribution imply  $e = 0.49 \pm 0.19$ .

For the case of two planet systems, the formalism produces simple analytic expressions for the parameters of the eccentricity distribution. The distribution itself can be derived by taking the solution of equation (6) and solving for the eccentricity as a function of time. Since time is distributed uniformly, the resulting expression can be solved for the corresponding distribution of eccentricity, which can then be written in the form

$$\frac{dP}{de} = \left[ 1 - \left( \frac{e^2 - \Lambda_{j1}^2 - \Lambda_{j2}^2}{2\Lambda_{j1}\Lambda_{j2}} \right)^2 \right]^{-1/2} \frac{e}{\pi\Lambda_{j1}\Lambda_{j2}}, \quad (7)$$

where  $\Lambda_{ji}$  are the eigenvectors. This form of the eccentricity distribution (for the  $j$ th planet) is valid between the extremes given by

$$e_{max}, e_{min} = |\Lambda_{j1} \pm \Lambda_{j2}|. \quad (8)$$

The mean value of the distribution can be evaluated from its definition  $\langle e \rangle = \int e(dP/de)de$  and takes the form

$$\langle e \rangle_j = (2/\pi)(\Lambda_{j1} + \Lambda_{j2})E(\hat{m}), \quad (9)$$

where  $E(\hat{m})$  is the elliptical integral of the second kind (Abramowitz & Stegun 1970) with parameter  $\hat{m} \equiv 4\Lambda_{j1}\Lambda_{j2}/(\Lambda_{j1} + \Lambda_{j2})^2$ . Notice that the parameter  $\hat{m}$  can be negative and hence care must be

taken in evaluating  $E(\hat{m})$ . The corresponding variance of the distribution is given by

$$\sigma_{ej}^2 = \Lambda_{j1}^2 + \Lambda_{j2}^2 - \frac{4}{\pi^2}(\Lambda_{j1} + \Lambda_{j2})^2[E(\hat{m})]^2. \quad (10)$$

For two-planet systems, we have verified that these expressions for the mean, extrema, and variance of the distribution are in good agreement with those found via sampling of the secular solutions as described above.

Figure 1 illustrates the effect of this eccentricity variation on the  $a - e$  plane. The bottom panel shows the locations of the planets in the  $a - e$  plane for our sub-sample of multiple planet systems, where the observed eccentricities are taken at face value. The top panel shows the same diagram with the observed eccentricity values replaced by the ranges of eccentricities predicted by secular theory. The relatively large (and previously unexpected) values of eccentricity found in the observational sample to date has led to an explosion of theoretical explanations (e.g., Ogilvie & Lubow 2003, Goldreich & Sari 2003, Adams & Laughlin 2003; Moorhead & Adams 2005). Secular interactions change the target of these investigations: Instead of explaining the observed distribution of eccentricity values (where the observed  $e$  are taken as given), a complete theory must provide an explanation of the underlying distribution of eccentricity from which the currently observed values are sampled.

The secular theory used here is derived from a disturbing function that is correct only to second order in eccentricity and inclination angle and first order in the planet masses (MD99). In order to test how well this version of secular theory describes the eccentricity evolution of these systems, we have performed a set of numerical integrations for a representative sub-sample of the extrasolar planetary systems. The time evolution of eccentricity is shown in Figures 2 – 4 for three representative systems in our sample (HD37124, HD168443, HD12661). For HD37124 and HD168443 (Figures 2 and 3), the time evolution predicted by secular theory is in good agreement with the numerical integrations, although not exact. For the HD12661 system, however, the eccentricity times series produced by secular theory does not provide an accurate description of that indicated by numerical integration. In addition, the numerical integration results depend sensitively on the initial conditions; Figure 4 shows the results of two sets of starting parameters (both within the observational errors). In spite of these complications, however, for all three of the systems, the amplitude of eccentricity variation predicted by secular theory is in good agreement with that predicted by direct numerical integration. Specifically, the envelopes of the eccentricity variations are in agreement. (Of course, an improved point-to-point time variation can be obtained with a higher order approximation scheme – see Lee & Peale 2003).

### 3.2. Possible Earth-like Planets in Extrasolar Planetary Systems

#### 3.2.1. Constraints from forced eccentricity oscillations

One of the themes of upcoming space missions (especially Terrestrial Planet Finder, hereafter TPF) is to detect Earth-like planets, with an emphasis on those in “habitable” Earth-like orbits. For solar mass stars, the standard scenario (Kasting et al. 1993) suggests that such orbits would have semi-major axes near  $a = 1$  AU and relatively low eccentricity (although the maximum eccentricity threshold is not well determined – see below). For the multiple planet systems discovered to date, the detected planets are of order Jovian mass, much larger than the mass of Earth. As a result, to first approximation, any putative Earth-like planets present in these systems can be considered as test particles. Within the framework of secular interactions considered here, we can calculate the effects of extant planets on hypothetical Earth-like planets (test bodies) that may reside in the systems. According to secular theory (MD99, §2), the motion of test particles can be characterized by a frequency  $A$  of free oscillation, which takes the form

$$A = n_0 \left[ \frac{1}{4} \sum_j \frac{m_j}{M_*} \alpha_{0j} \bar{\alpha}_{0j} b_{3/2}^{(1)}(\alpha_{0j}) + 3 \frac{GM_*}{c^2 a_0} \right], \quad (11)$$

where the subscript ‘0’ refers to the orbit of the test particle and where the rest of the symbols have the same meaning as in the previous section. Notice that the free oscillation frequency  $A$  is a function of the test particle semi-major axis  $a_0$ .

By applying the formalism described above to extant systems with multiple giant planets, we can explore the forced oscillations of any additional small (e.g., terrestrial) planets. The results are shown in Figures 5 – 9 for a collection of observed systems. This subset was chosen to include systems that experience nontrivial secular interactions, but still might allow for a habitable planet (HD38529, HD74156, HD168443). Other systems (not shown) either have little secular interaction or already have a planet near  $a \sim 1$  AU (we consider HD12661 as an example of this latter type of system). The bottom panels of these figures show the free oscillation frequency  $A$ , plotted as a function of possible semi-major axis  $a_0$ , for hypothetical test bodies in the given extrasolar planetary systems.

A related quantity is the amplitude of forced eccentricity oscillations; these amplitudes are plotted as a function of semi-major axis in the top panels of Figures 5 – 9. Briefly, the eccentricity of a test particle at any given time is the vector sum of the forced eccentricity and the free eccentricity (see Fig. 7.2 of MD99). The amplitude of forced eccentricity oscillation is determined by the semi-major axis of the test particle and the secular solution for the perturbing bodies; it varies over secular time scales, as the perturbing planets interact with each other. The free eccentricity is determined by the boundary conditions and represents a more “fundamental” orbital parameter (for further detail see MD99). The amplitudes shown in the figures are calculated for the starting time  $t = 0$ , i.e., with the current values of the orbital elements. Over time, the amplitude curve oscillates and thereby gives an effective width to the curve.

For the systems HD38529, HD74156, HD168443, and HD37124 (Figs. 5 – 8), the theory of secular interactions predicts that Earth-like planets (small bodies with semi-major axes near 1 AU) can reside in the planetary systems [both  $A$  and  $e(\text{forced})$  are small]. However, the forced eccentricities of the planets are appreciably larger than that of Earth, specifically in the range  $e(\text{forced}) \approx 0.10 - 0.30$ . In addition, the outer planets pose a threat to long term stability in these systems. Extrapolation of the results of numerical integrations (David et al. 2003) indicates that an Earth-like planet can remain stable over the current 4.6 Gyr age of the Solar System for a Jupiter mass companion with periastron  $a(1 - e) \gtrsim 2.55$  AU. However, even the largest periastron value in this sample of systems is somewhat lower,  $\sim 2.5$  AU for HD38529, suggesting that long term stability may be a problem (a host of papers have considered long term stability of observed extrasolar planetary systems, including Érdi et al. 2004; Menou & Tabachnik 2003; Noble et al. 2002; Jones et al. 2001; and many others). Indeed, simulations of extrasolar planetary systems with added massless test particles (Barnes & Raymond 2004) indicate that small values of forced eccentricity (Figs. 5 – 8) are necessary but not sufficient; these simulations show that HD74156 and HD168443 eject almost all of the test particles in a few Myr, while HD38529 and HD37124 allow for continued particle survival.

### 3.2.2. Mean yearly flux versus eccentricity

An important (unresolved) question is the maximum allowed eccentricity for a “habitable” planet. Such planets are generally assumed to have nearly circular orbits. In planetary systems with detectable giant planets, however, any possible terrestrial planets are likely to be subject to eccentricity forcing and hence nonzero mean values of  $e$ . Although the details of habitability must ultimately depend on the characteristics of the planetary atmosphere, and such a discussion is beyond the scope of this paper, the variations in the stellar flux are straightforward to determine. For nonzero eccentricities, the flux received by the planet cannot be described by a single value, like the well-known value of our solar constant  $1.36 \times 10^6 \text{ erg sec}^{-1} \text{ cm}^{-2}$ , but rather a distribution of values. We can determine the parameters of this distribution. Let  $F_0$  be a fiducial value of the flux defined by

$$F_0 \equiv \frac{L_*}{4\pi a^2}. \quad (12)$$

In other words,  $F_0$  is the value of the (constant) flux received by a planet on a circular orbit of radius  $a$ . The extrema of the distribution are then given by  $F_{max} = F_0/(1 - e)^2$  and  $F_{min} = F_0/(1 + e)^2$ . If we define a reduced flux  $f = F/F_0 = (a/r)^2$ , the distribution of reduced flux can be written in the form

$$\frac{dP}{df} = \frac{1}{2\pi f^{3/2}} [2\sqrt{f} - 1 - f(1 - e^2)]^{-1/2}. \quad (13)$$

The time-averaged mean value of the flux is then given by

$$\langle F \rangle = \frac{F_0}{(1 - e^2)^{1/2}}. \quad (14)$$



The requirement of a given mean flux (averaged over the planet’s year) thus demands that the quantity  $a^2\sqrt{1-e^2}$  attain a particular value, in contrast to the particular value of  $a$  usually required for circular orbits. Notice also that with increasing eccentricity, the mean flux is larger for a given semi-major axis, or, equivalently, the planet can live farther from its star. The variance (width)  $\sigma_F$  of the distribution can be written in the form

$$\sigma_F = \langle F \rangle \left[ \frac{1 + e^2/2}{(1 - e^2)^{3/2}} - 1 \right]^{1/2}, \quad (15)$$

so that the distribution of flux experienced by the planet grows wider with increasing eccentricity (as expected).

Highly eccentric orbits will produce large seasonal variations on the planet (in addition to those produced by possible tilting of the spin axis) and it remains to be determined how large such variations can be and still allow for a habitable world. Sufficiently large eccentricities lead to nonlinear seasonal flux variations. One useful benchmark occurs for the case  $\sigma_F = \langle F \rangle$ , where the flux distribution is as wide as its mean, which in turn occurs for eccentricity  $e_0 \approx 0.554$ . With this eccentricity, the yearly flux varies by a factor of  $\sim 12$  from maximum to minimum. As another benchmark, even a modest eccentricity of  $e \approx 0.172$  will enforce a factor of two variation in flux over the planetary orbit. Although the flux variations are straightforward to calculate, the degree to which planets can maintain stable climates in the face of such variations remains to be determined. In any case, these considerations have important implications for astrobiology (e.g., Lunine 2005).

Keep in mind that the distributions of flux considered here are the possible values of flux experienced by the planet over the course of its “year” for a given eccentricity. Over longer time scales, those determined by secular interactions, the eccentricity itself will sample a distribution of values as discussed in the previous subsection.

### 3.3. General Relativity in Extrasolar Planetary Systems

The combination of secular interactions and general relativity provides a number of interesting results. For some extrasolar planetary systems, one can use observed system parameters to provide new tests of general relativity; in other systems, one can use general relativity to place new physical constraints on the system parameters (see also Adams & Laughlin 2006b).

In order for the effects of general relativity to be significant, the final term in equation (4) must compete with the others. In practice, only the inner planet will have significant corrections. To find an analytic criterion for the importance of relativistic effects, we assume that the system is sufficiently hierarchical so that  $b_{3/2}^{(1)}(\alpha_{j0}) = 3\alpha_{j0} + \mathcal{O}(\alpha_{j0}^2) \approx 3\alpha_{j0}$  and thus obtain the requirement

$$\sum_j \frac{m_j}{M_*} \alpha_{j0}^3 \sim \frac{4GM_*}{c^2 a_0}. \quad (16)$$

Both sides of this equation are small dimensionless quantities; however, when their ratio is of order unity, then relativistic effects can compete with secular interactions. Since in most cases, only one of the (non-inner) planets will contribute to the sum on the left hand side of the equation, this constraint is equivalent to the requirement that one of the dimensionless fields  $\Pi_j \gtrsim 1$ , where

$$\Pi_j \equiv \frac{4GM_*^2 a_j^3}{c^2 m_j a_0^4} \approx 6.3 \left(\frac{m_j}{m_J}\right)^{-1} \left(\frac{M_*}{M_\odot}\right)^2 \left(\frac{a_j}{1 \text{ AU}}\right)^3 \left(\frac{a_0}{0.05 \text{ AU}}\right)^{-4}. \quad (17)$$

The second (approximate) equality indicates that relativistic effects compete with non-relativistic secular interactions for a Jupiter mass planet in a 1 AU orbit perturbing a hot Jupiter (in a 4 day orbit). The relative size of the relativistic effect grows with increasing semi-major axis  $a_j$  of the perturber, but the magnitude of the secular contribution decreases.

This problem also contains a characteristic time scale  $\tau_{\text{gr}}$  defined by

$$\tau_{\text{gr}} \equiv \frac{c^2 a_0^{3/2}}{3(GM_*)^{3/2}} \approx 3011 \text{ yr} \left(\frac{a_0}{0.05 \text{ AU}}\right)^{5/2} \left(\frac{M_*}{1.0 M_\odot}\right)^{-3/2}. \quad (18)$$

This scale represents the time required for the periastron of a hot Jupiter (in about a 4-day orbit) to precess one radian forward in its orbit. Notice that this time scale is comparable to the secular interaction time scales (determined by the Laplace-Lagrange eigenvalues) shown in Table 1 for many of the observed systems. This concordance of time scales,  $\tau_{\text{gr}} \sim \tau_{\text{sec}}$ , is purely accidental (in that a different value of the speed of light  $c$  would change the result, and planetary system formation probably does not depend on relativistic effects) but allows for GR to play a significant role in the dynamics of some planetary systems.

To illustrate the action of relativity in extrasolar planetary systems, we have calculated the secular interactions for two systems with and without including the general relativistic terms. We use the systems Upsilon Andromedae and HD160691 because they contain hot Jupiters as well as additional planets in orbits with  $a \sim 1$  AU. Figure 10 shows the mean eccentricity  $\langle e \rangle$  of the innermost planet, as driven by secular interactions and averaged over many cycles, plotted as a function of  $\sin i$  for the two cases.

For the Upsilon Andromedae system (top panel of Fig. 10), the inclusion of relativity acts to damp the excitation of eccentricity by secular interactions. For large values of  $\sin i$ , the innermost planet would be driven to eccentricity values  $\langle e \rangle \approx 0.4$  without relativity, but only  $\langle e \rangle \approx 0.016$  when the relativistic corrections are included. The observed eccentricity for the inner planet in this system is  $e_{\text{obs}} \sim 0.011$ , much closer to the relativistic mean value. As a result, one can think of Upsilon Andromedae as providing another test of general relativity. Since secular theory uses the current (observed) eccentricity values of the planets as part of the boundary conditions, the system always has a chance of displaying the observed (low) eccentricity of the inner planet, so the implications for general relativity must be stated in terms of probabilities: If we assume that the observed eccentricity of the inner planet has a measurement error that is gaussian distributed with  $\sigma_{\text{obs}} = 0.015$ , then the probability of observing the system in its current state would be only

0.0235 if the general relativistic corrections are not included. An analogous calculation implies a probability of 0.78 of finding the inner planet with its observed eccentricity if general relativity is correct. The validity of GR is thus strongly favored.

For the HD160691 system (bottom panel of Fig. 10), the inclusion of relativistic terms acts in the opposite direction, i.e., it leads to greater predicted values of  $\langle e \rangle$ . For large values of  $\sin i \sim 1$ , the predicted mean driven eccentricities are small enough to be consistent with the observed low value  $e_{obs} \sim 0$ . As the value of  $\sin i$  decreases, however, the level of eccentricity forcing increases and reaches a resonance near  $\sin i \approx 0.5$ . The observed low value of eccentricity, in conjunction with these considerations, thus constrain the viewing angle of the HD160691 system to be nearly edge-on; if we require  $\langle e \rangle \lesssim 0.05$ , then the viewing angle is confined to the range  $\sin i \gtrsim 0.93$  ( $i \gtrsim 70^\circ$ ). Since inclination angles are notoriously difficult to measure in these systems, this constraint on  $i$  is quite valuable.

This constraint on the viewing angle also has implications for the possibility of observing the inner planet in transit. For a hot Jupiter in a zero eccentricity orbit, the *a priori* probability  $\mathcal{P}_0$  that the planet can be seen in transit is given by

$$\mathcal{P}_0 = \frac{\int_0^{(R_*+r_P)/a} d(\cos i)}{\int_0^1 d(\cos i)} = \frac{R_* + R_P}{a}. \quad (19)$$

For the HD160691 system, the inclination angle is confined to the narrower range  $\sin i \gtrsim 0.93$  ( $\cos i \lesssim 0.37$ ) and the probability that the inner planet can be seen in transit is larger than the *a priori* value by a factor of 2.7. With this constraint on the inclination angle, the probability of finding observable transits in HD160691 is  $\mathcal{P} \sim 0.14$ , making it one of the higher probability systems<sup>2</sup>.

Most previous discussions of relativistic effects in planetary systems emphasize its stabilizing influence. However, general relativity can lead to either larger eccentricity forcing (HD160691) and hence less stability, or smaller eccentricity forcing (Ups And) and hence greater stability (Adams & Laughlin 2006b). It is useful to have an analytic criterion for when the two types of behavior occur, and what system parameters are required for GR to provide more/less stability.

For a two planet system, we can isolate the effects of relativity by considering the simplest case in which the inner planet has a nearly circular orbit, or at least cycles through the  $e_1 = 0$  state. This case is relatively common in that close planets tend to have nearly circular orbits and close planets display relativistic effects. The solution of equation (6) can be used to find the square of the eccentricity of the inner planet. After time averaging, the resulting amplitude can be written in terms of the eigenvectors so that  $\langle e_1^2 \rangle = \eta^2 = \Lambda_{11}^2 + \Lambda_{12}^2$ . By finding the eigenvectors in terms of the original matrix elements  $A_{ij}$  and applying the boundary conditions, we can write the eccentricity

---

<sup>2</sup>www.transitsearch.org

amplitude of the inner planet (as forced by the outer planet) in the form

$$\eta^2 = \frac{A_{12}^2 e_{02}^2}{(\lambda_1 - \lambda_2)^2}, \quad (20)$$

where  $e_{02}$  is the initial eccentricity of the second (outer) planet (see the following subsection). For a two planet system, the difference in eigenvalues is given by the expression

$$\lambda_1 - \lambda_2 = [(A_{11} - A_{22})^2 + 4A_{12}A_{21}]^{1/2}, \quad (21)$$

which is positive definite. Notice that the eigenvalues cannot be degenerate for a two planet system, and hence secular interactions do not lead to resonance. Notice also that only the diagonal matrix elements contain relativistic corrections, and only the inner planet is generally close enough to the star for such corrections to make a difference. The first matrix element can thus be written

$$A_{11} = A_0 + 3n_1\mu, \quad (22)$$

where  $A_0$  is the matrix element in the absence of relativity and  $\mu = GM_*/(c^2 a_1)$  is the dimensionless relativistic correction factor. With this construction, the question of whether relativity acts to enforce larger or smaller amplitudes of eccentricity oscillation is determined by the sign of the derivative  $d\eta/d\mu$ . In order to outline its dependence on the system parameters, we make the same approximations as before ( $m_1, m_2 \ll M_*$ ;  $a_1 \ll a_2$  so that  $b_{3/2}^{(1)} \approx 3a_1/a_2$ ; etc.) and write the derivative in the form

$$\text{sign}\left(\frac{d\eta}{d\mu}\right) = -\text{sign}\left[1 + \Pi - \frac{m_1}{m_2}\left(\frac{a_1}{a_2}\right)^{1/2}\right], \quad (23)$$

where  $\Pi$  is the dimensionless field defined in equation (17). The third term must dominate in order for the sign to be positive, and hence for relativity to lead to greater eccentricity amplitudes. Since  $a_1 < a_2$  by definition, and since the inner planets tend to be less massive ( $m_1 < m_2$ ), relativity will usually lead to greater stability. For sufficiently massive inner planets, however, relativity can amplify eccentricity forcing. One convenient way to write the constraint (requirement) for eccentricity amplification is in the form

$$m_2 < m_1\left(\frac{a_1}{a_2}\right)^{1/2} - 4\mu M_*\left(\frac{a_1}{a_2}\right)^{-3}. \quad (24)$$

Keep in mind that we are working in the limit  $a_1 \ll a_2$ , which is also required for long term dynamical stability. As a result, this constraint cannot, in practice, be satisfied by making the ratio  $a_1/a_2$  too large; instead, the mass  $m_2$  must be small compared with  $m_1$ . The two planet systems considered in this paper (Table 2) show an interesting trend: None of the systems satisfy the inequality of equation (24), so that general relativity leads to greater stability for all of these systems.

Now consider a three planet system in which the inner planet has relatively little effect on the outer two planets, due to its smaller mass and/or inner position (far from the others). This description applies to both HD160691 and UpsAnd. In this hierarchical limit, the  $3 \times 3$  matrix

$A_{ij}$  can be approximated by taking  $A_{12} = A_{13} = A_{21} = A_{31} = 0$ . The eigenvalues of this reduced matrix then take the form

$$\lambda_1 = A_{11}, \lambda_{2,3} = \frac{1}{2} \{ (A_{22} + A_{33} \pm [(A_{33} - A_{22})^2 + 4A_{23}A_{32}]^{1/2}) \}. \quad (25)$$

With this level of complexity, the system can have degenerate eigenvalues, e.g., when  $\lambda_1 = A_{11}$  is equal to either  $\lambda_2$  or  $\lambda_3$ . Without loss of generality, suppose that  $\lambda_1$  and  $\lambda_2$  are nearly degenerate. The effect of general relativity is to add a small positive contribution to  $A_{11}$  and hence  $\lambda_1$  (we again take  $A_{11} = A_0 + 3n_1\mu$ ), where the physical implication of the added term is the general relativistic precession of the orbit of the inner planet. If  $\lambda_1 \lesssim \lambda_2$ , then GR brings the eigenvalues closer together and thus acts to increase the level of eccentricity forcing. If  $\lambda_1 \gtrsim \lambda_2$ , then GR makes the eigenvalues more unequal and acts to decrease eccentricity forcing. The full cubic equation for  $\det[A - \lambda I]$  is more complicated, but allows for similar behavior.

The basic result of this section is that general relativity can have a significant effect on secular perturbations for planetary systems with favorable characteristics (see also Holman et al. 1997; Ford et al. 2000ab). The requirement that GR effects are important is quantified by the dimensionless field defined in equation (17). Furthermore, general relativity can either enhance or attenuate the effects of secular perturbations, where the sign of the relativistic effects is described by equations (20 – 25).

### 3.4. Constraints on Additional Planets in Systems with Hot Jupiters

Most hot Jupiters are observed to have small or zero eccentricity values and relatively low mass. For those systems that have observed hot Jupiters but no additional planets detected (thus far), the theory of secular interactions places a clean constraint on any possible companions. The presence of any additional planet (or larger body) will tend to excite eccentricity in the hot Jupiter. For the case of interest, we can set  $e_1(t = 0) = 0$  (the hot Jupiter is observed in a circular orbit) and  $\varpi_2(t = 0) = 0$  (we choose the orientation of the coordinate system so that the possible companion planet has zero argument of periastron). With these simplifications, the enforced eccentricity of the inner planet (the hot Jupiter) samples a distribution characterized by the following parameters:

$$e_{min} = 0, \quad e_{max} = 2\eta, \quad \langle e \rangle_1 = \frac{4}{\pi}\eta, \quad \langle e_1^2 \rangle = 2\eta^2, \quad \text{and} \quad \sigma_1^2 = [2 - 16/\pi^2]\eta^2, \quad (26)$$

where the amplitude  $\eta$  is defined in terms of the eccentricity  $e_{2(obs)}$  of the second planet and the matrix elements  $A_{ij}$ , i.e.,

$$\eta^2 \equiv \frac{A_{12}^2}{(A_{11} - A_{22})^2 + 4A_{12}A_{21}} e_{2(obs)}^2. \quad (27)$$

With this formulation, we can find the orbital elements of a second planet that would drive the eccentricity of the hot Jupiter to a specified mean value  $\langle e \rangle_1$ . Figure 11 shows the resulting  $a - e$  plane for the orbital elements of the (hypothetical) second planet. For example, the lowest curve

shows the required eccentricity  $e_2$  of the second planet as a function of its semi-major axis  $a_2$  such that the inner planet is excited to have a mean eccentricity  $\langle e \rangle_1 = 0.01$ . The shaded region below this curve depicts the portion of parameter space for which the second planet has a negligible effect on the hot Jupiter. The corresponding curves for  $\langle e \rangle_1 = 0.02, 0.05, 0.10, 0.20,$  and  $0.50$  are also shown. The observed hot Jupiters do not have companions in the unshaded region of the plane. However, such planets could exist – the square symbols in Figure 11 depict the locations of known planets in the  $a - e$  plane. Notice that the relevant portion of the  $a - e$  plane is relatively small. The curves shown in Figure 11 assume that the hot Jupiter has a period of 4 days and the minimum period of the second planet is 12 days, just outside the 3:1 mean motion resonance (i.e., wide enough separations so that we expect secular theory to apply). The eccentricity  $e_2$  required to drive a given  $\langle e \rangle_1$  grows rapidly with increasing semi-major axis (period) and exceeds unity for relatively modest values of  $a_2$  as shown in the figure. Of course, the eccentricity of the inner planet cycles through a distribution of values. For this case, the cumulative probability  $\mathcal{P}(e)$  that the inner planet is observed with an eccentricity  $e_{obs} < e$ , for a system with mean (forced) eccentricity  $\langle e \rangle_1$ , is given by the expression

$$\mathcal{P}(e) = \frac{2}{\pi} \sin^{-1} \left( \frac{2e}{\pi \langle e \rangle_1} \right). \quad (28)$$

This form can be derived by evaluating the probability distribution of equation (7) for the case under consideration (where  $\Lambda_{11} = \Lambda_{12} = \eta$ ) and performing the integral to find the cumulative probability.

#### 4. Conclusion

This paper has applied the leading order theory of secular interactions to observed extrasolar planetary systems and used the results to constrain their properties. Our results can be summarized as follows:

[1] Through dynamical interactions, described here using secular theory, the orbital eccentricities in multiple planet systems vary over secular time scales. The eccentricities measured by ongoing planet searches represent the current eccentricity value, which is drawn from a wider distribution of values sampled by the planet. In other words, the eccentricities in multiple planet systems should not be considered as particular values, but rather as distributions of values. The widths of these eccentricity distributions can be substantial (Tables 2 and 3) and we have verified that secular theory predicts distribution widths that are in good agreement with direct numerical integration (Figures 2 – 4). This effect implies that interpretations of the  $a - e$  diagram must be regarded with caution for multiple planet systems (see Figure 1). For the simplest case of two planet systems, the resulting distribution of eccentricity can be found analytically (eqs. [7 – 10]). The time scale for secular eccentricity variations is typically thousands of years (Table 1), much longer than observational survey time scales (tens of years) and much shorter than the system lifetimes (few Gyr).

[2] For a sub-sample of observed multiple planet systems, we have calculated the frequencies of free oscillation and amplitudes of forced eccentricity oscillation (Figures 5 – 9) for (hypothetical) test bodies. These results constrain the possibility of multiple planet systems containing additional small (terrestrial) planets. This calculation shows that many of the systems allow the existence of additional planets, but the forced eccentricity amplitudes would be large compared to that of Earth, i.e.,  $e(\text{forced}) \approx 0.10 - 0.15$ . In addition, numerical integrations (Barnes & Raymond 2004) indicate that only a fraction of these systems allow test bodies to remain stable over long time scales, i.e., the condition of small forced eccentricity amplitude is necessary but not sufficient.

[3] This paper generalizes the concept of a habitable zone to include the possibility of larger eccentricity values (§3.2.2). Specifically, we have calculated the distribution of flux experienced by a planet in an eccentric orbit over the course of its year (eq. [13]), as well as the mean flux and the width of the distribution (eqs. [12 – 15]). Notice that all of these results are calculated analytically.

[4] For multiple planet systems with favorable architectures, the effects of general relativity can be significant (Fig. 10). When planetary systems have two relatively massive outer planets and a third inner planet of smaller mass near secular resonance, the effects of general relativity are large enough to move the system in or out of a resonant condition. Since the resonance condition depends on planetary masses, which in turn depend on  $\sin i$ , and since small inner planets cannot survive in exact resonance, this effect can be used to constrain the allowed range of  $\sin i$  in some observed extrasolar planetary systems. For the HD160691 system, e.g., this constraint implies that  $\sin i \gtrsim 0.93$ . This effect thus provides another means of probing the properties of these planetary systems. For other systems (e.g., Upsilon Andromedae), general relativity can make the inner planet precess forward in its orbit fast enough to compromise eccentricity pumping from a second planet, i.e., the mean eccentricity values are much smaller than they would be in flat space. This latter effect can thus be used as a test of general relativity. For Ups And, the system has a 78% chance of being observed with its measured parameters if general relativity is correct, but only a  $\sim 2\%$  chance if the general relativistic corrections were zero. In the future, additional extrasolar planetary systems and/or higher precision observations can provide more stringent tests of GR (see also Adams & Laughlin 2006b).

[5] For single planet systems with small or zero measured eccentricity values (e.g., 51 Peg), the small observed  $e$  values imply the absence of large, close planetary companions. For a given system, this line of reasoning implies a limit on the possible orbital elements of any additional planets in the system (shown in Fig. 11).

The objective of this paper is to outline the effects of secular interactions in multiple planet systems. We have applied the results to a small collection of multiple planet systems that have been detected, and a number of additional applications are expected in the near future. Although the sample of extrasolar planets ( $\sim 150$ ) is now large enough to provide some statistical significance, the number of multiple planet systems is still low ( $\sim 20$ ). Furthermore, the possible parameter space accessible to multi-planet systems is enormous, so it is premature to make statistical state-

ments about multiple planet systems. Nonetheless, future observations will find greater numbers of systems with multiple giant planets (through continued radial velocity searches and other methods) and systems containing smaller, Earth-mass planets (e.g., TPF).

Secular interactions can add to our understanding of these forthcoming multiple planet systems in a variety of ways. In trying to find theoretical explanations for the observed orbital elements, one must take into account the distributions of eccentricities driven by secular interactions (Fig. 1). In systems with known giant planets, the search for Earths can be guided by studying the forced eccentricity variations as depicted in Figures 5 – 9. Some multiple planet systems will provide additional (stronger) tests of general relativity (as in Fig. 10). In other systems, we can deduce the presence or absence of additional (undetected) planets — or at least constrain their properties — through examination of the properties of the detected planets (Fig. 11). Over longer time spans, secular interactions combine with tidal circularization and energy dissipation processes (as outlined in our companion paper Adams & Laughlin 2006a).

This work was supported at U. Michigan (FCA) by the Michigan Center for Theoretical Physics and by NASA through the Terrestrial Planet Finder Mission (NNG04G190G) and the Astrophysics Theory Program (NNG04GK56G0). This material is based in part upon work supported by the National Science Foundation CAREER program under Grant No. 0449986 (GL), and was also supported at U. C. Santa Cruz (GL) by NASA through the Terrestrial Planet Finder Precursor Science Program (NNG04G191G) and through the Origins of Solar Systems Program (NAG5-13285).



## REFERENCES

- Abramowitz, M., & Stegun, I. A. 1970, Handbook of Mathematical Functions (New York: Dover)
- Adams, F. C., & Laughlin, G. 2003, *Icarus*, 163, 290
- Adams, F. C., & Laughlin, G. 2006a, submitted to *ApJ*
- Adams, F. C., & Laughlin, G. 2006b, submitted to *Grav. Res. Found. Essays on Gravitation*
- Barnes, R., & Raymond, S. N. 2004, *ApJ*, 617, 569
- Brouwer, D. & van Woerkom, A.J.J. 1950, *Astron. P. Amer. Ephem.*, 13, 81
- Butler, R. P., Marcy, G. W., Fischer, D. A., Brown, T. M., Contos, A. R., Korzennik, S. G., Nisenson, P., & Noyes, R. W. 1999, *ApJ*, 526, 916
- David, E. M., Quintana, E. V., Fatuzzo, M., & Adams, F. C. 2003, *PASP*, 115, 825
- Érdi, B., Dvorak, R., Sádnor, Zs., Pilat-Lohinger, E., & Funk. B. 2004, *MNRAS*, 351, 1043
- Ford, E. B., Kozinsky, B., & Rasio, F. A. 2000a, *ApJ*, 535, 385
- Ford, E. B., Joshi, K. J., Rasio, F. A., & Zbarsky, B. 2000b, *ApJ*, 528, 336
- Goldreich, P., & Sari, R. 2003, *ApJ*, 585, 1024
- Holman, M., Touma, J., & Tremaine, S. 1997, *Nature*, 386, 254
- Jones, B. W., Sleep, P. N., Chambers, J. E. 2001, *A&A*, 366, 254
- Kasting, J. F., Whitmire, D. P., & Reynolds, R. T. 1993, *Icarus*, 101, 108
- Laskar, J. 1988, *A & A*, 198, 341
- Lee, M. H., & Peale, S. J. 2003, *ApJ*, 592, 1201
- Lubow, S. H., & Ogilvie, G. I. 2001, *ApJ*, 560, 997
- Lunine, J. I. 2005, *Astrobiology: A Multidisciplinary Approach* (San Francisco: Pearson Educational Press)
- Marcy, G., & Butler, P. R. 1996, *ApJ*, 464, L147
- Mardling, R. A., & Lin, D.N.C. 2002, *ApJ*, 573, 829
- Mardling, R. A., & Lin, D.N.C. 2004, *ApJ*, 614, 955
- Mayor, M., & Queloz, D. 1995, *Nature*, 378, 355

- Menou, K., & Tabachnik, S. 2003, *ApJ*, 583, 473
- Michtchenko, T. A., & Malhotra, R. 2004, *Icarus*, 168, 237
- Moorhead, A. V., & Adams, F. C. 2005, *Icarus*, 178, 517
- Murray, C. D., & Dermott, S. F. 1999, *Solar System Dynamics* (Cambridge: Cambridge Univ. Press) (MD99)
- Nagasawa, M., Lin, D.N.C., & Ida, S. 2003, *ApJ*, 586, 1374
- Noble, M., Musielak, Z. E., Cuntz, M. 2002, *ApJ*, 572, 1024
- Ogilvie, G. I., & Lubow, S. H. 2003, *ApJ*, 587, 398
- Rivera, E. J. et al. 2005, *ApJ*, 634, 625
- Takeda, G., & Rasio, F. A. 2005, *ApJ*, 627, 1001
- Wu, Y., & Goldreich, P., 2002, *ApJ*, 564, 1024

**Table 1: Secular Time Scales**

System	$\tau_1$ (yr)	$\tau_2$ (yr)	$\tau_3$ (yr)	$\tau_4$ (yr)
GJ876	81.6	53.2	4.4	–
55Cnc	4030000	369	73.3	40.9
UpsAnd	4880	1924	1042	–
HD217107	2865500	7198	–	–
HD160691	9431	6734	2069	–
HD38529	1953000	10490	–	–
HD190360	21055000	28360	–	–
HD11964	2118390	52260	–	–
HD74156	118290	9308	–	–
HD168443	13100	1837	–	–
HD37124	4918	2735	1047	–
HD73526	386	55.6	–	–
HD82943	551	78.9	–	–
HD169830	12496	3603	–	–
HD202206	2130	396	–	–
HD12661	5501	2407	–	–
HD108874	6311	2261	–	–
HD128311	567	79	–	–
47UMa	5520	818	–	–

**Table 2: Eccentricity Variations from Secular Theory  
(systems with 2 planets)**

System	$m_P(m_J)$	$a$ (AU)	$e_{obs}$	$\langle e \rangle$	$\sigma_e$	$e_{min}$	$e_{max}$
HD217107 b	1.369	0.074	0.130	0.130	0.0002	0.130	0.131
HD217107 c	1.846	3.681	0.670	0.670	0.0000	0.670	0.670
HD38529 b	0.783	0.129	0.275	0.274	0.0012	0.273	0.276
HD38529 c	12.818	3.714	0.330	0.330	0.0000	0.330	0.330
HD190360 c	0.062	0.128	0.010	0.117	0.0498	0.010	0.168
HD190360 b	1.519	3.867	0.380	0.380	0.0000	0.380	0.380
HD11964 b	0.116	0.230	0.150	0.148	0.0017	0.145	0.150
HD11964 c	0.699	3.171	0.300	0.300	0.0001	0.300	0.300
HD74156 b	1.858	0.294	0.635	0.617	0.0421	0.544	0.668
HD74156 c	6.453	3.446	0.561	0.563	0.0038	0.558	0.569
HD168443 b	7.784	0.295	0.529	0.538	0.0236	0.505	0.572
HD168443 c	17.311	2.862	0.228	0.225	0.0082	0.212	0.236
HD73526 b	2.039	0.652	0.390	0.382	0.0322	0.335	0.426
HD73526 c	2.261	1.039	0.400	0.404	0.0217	0.373	0.434
HD82943 b	1.856	0.746	0.380	0.295	0.1050	0.120	0.426
HD82943 c	1.848	1.179	0.180	0.242	0.1056	0.051	0.369
HD169830 b	2.881	0.812	0.310	0.357	0.0836	0.224	0.468
HD169830 b	4.057	3.598	0.330	0.308	0.0323	0.259	0.353
HD202206 b	16.786	0.811	0.435	0.416	0.0256	0.379	0.452
HD202206 c	2.348	2.499	0.267	0.340	0.1382	0.095	0.508
HD12661 b	2.339	0.822	0.330	0.305	0.0535	0.222	0.373
HD12661 c	1.573	2.661	0.200	0.217	0.0618	0.123	0.299
HD108874 b	1.386	1.042	0.130	0.298	0.1013	0.129	0.424
HD108874 c	0.992	2.729	0.380	0.249	0.1075	0.060	0.380
HD128311 b	2.475	1.077	0.210	0.265	0.1093	0.073	0.399
HD128311 c	3.168	1.723	0.270	0.203	0.0890	0.043	0.311
47UMa b	2.545	2.094	0.061	0.070	0.0133	0.050	0.088
47UMa c	0.764	3.735	0.100	0.074	0.0350	0.002	0.114

**Table 3: Eccentricity Variations from Secular Theory**  
(systems with 3 or 4 planets)

System	$m_P(m_J)$	$a$ (AU)	$e_{obs}$	$\langle e \rangle$	$\sigma_e$	$e_{min}$	$e_{max}$
GJ876 d	0.019	0.021	0.000	0.013	0.0060	0.000	0.020
GJ876 c	0.567	0.130	0.217	0.189	0.0209	0.158	0.217
GJ876 b	1.913	0.208	0.001	0.046	0.0221	0.001	0.072
55Cnc e	0.045	0.038	0.174	0.185	0.0631	0.043	0.301
55Cnc b	0.827	0.115	0.061	0.128	0.0608	0.009	0.203
55Cnc c	0.173	0.241	0.493	0.430	0.0552	0.347	0.506
55Cnc d	3.746	5.526	0.251	0.251	0.0000	0.251	0.251
UpsAnd b	0.686	0.059	0.011	0.016	0.0062	0.002	0.027
UpsAnd c	1.913	0.842	0.268	0.177	0.0812	0.025	0.274
UpsAnd d	3.760	2.527	0.270	0.288	0.0135	0.268	0.306
HD160691 d	0.046	0.090	0.000	0.035	0.0136	0.000	0.051
HD160691 b	1.669	1.500	0.200	0.489	0.1931	0.156	0.727
HD160691 c	3.135	4.170	0.570	0.496	0.0576	0.411	0.574
HD37124 b	0.710	0.546	0.071	0.130	0.0487	0.026	0.203
HD37124 c	0.695	1.743	0.170	0.115	0.0527	0.009	0.187
HD37124 d	0.739	3.078	0.100	0.108	0.0395	0.024	0.179

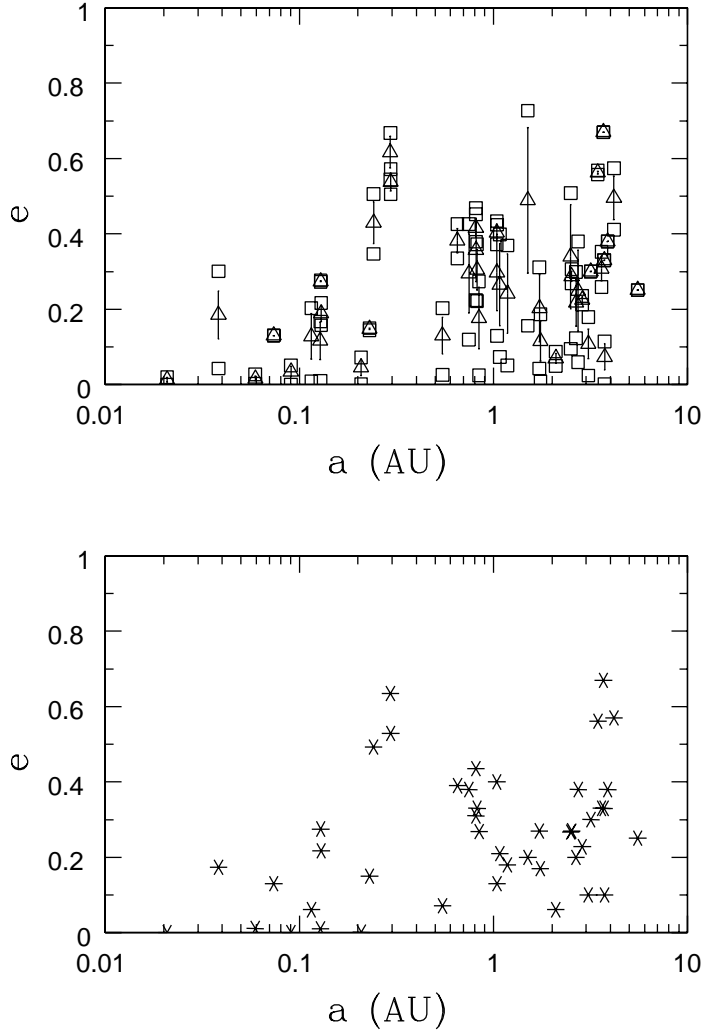


Fig. 1.— The effects of secular interactions on the  $a - e$  plane for observed multiple planet systems. The bottom panel shows the  $a - e$  plane using the observed eccentricities for all of the planets found in multiple systems (to date). The top panel shows the eccentricities predicted by Laplace-Lagrange secular theory for the same planets. The mean values of the eccentricity, averaged over many secular cycles, are shown as open triangles. The errorbars depict the range of eccentricities over the same cycles, as measured by the variance of the distribution, and the open squares depict the minimum and maximum values.

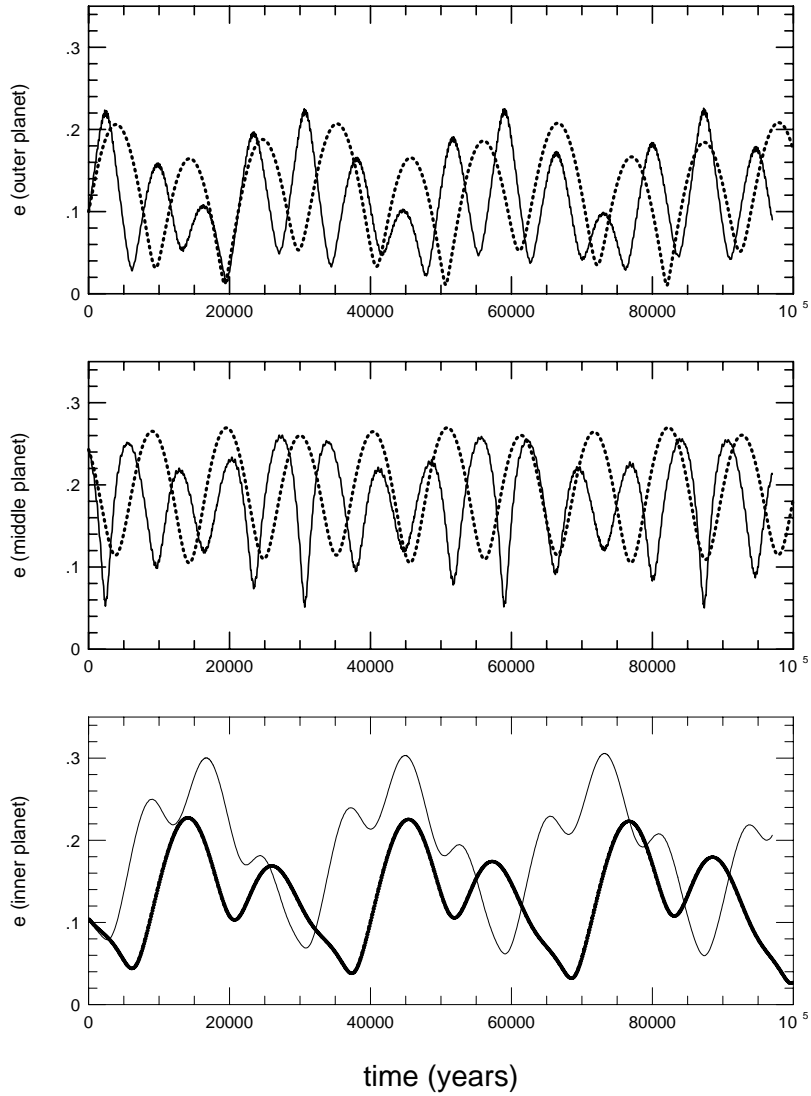


Fig. 2.— Comparison of secular theory with direct numerical integration for extrasolar planetary system HD37124. The eccentricity variations produced by direct numerical integration are shown by the solid curves; the corresponding eccentricity variations predicted by secular theory are shown by the dotted curves. The two approaches are in good agreement.

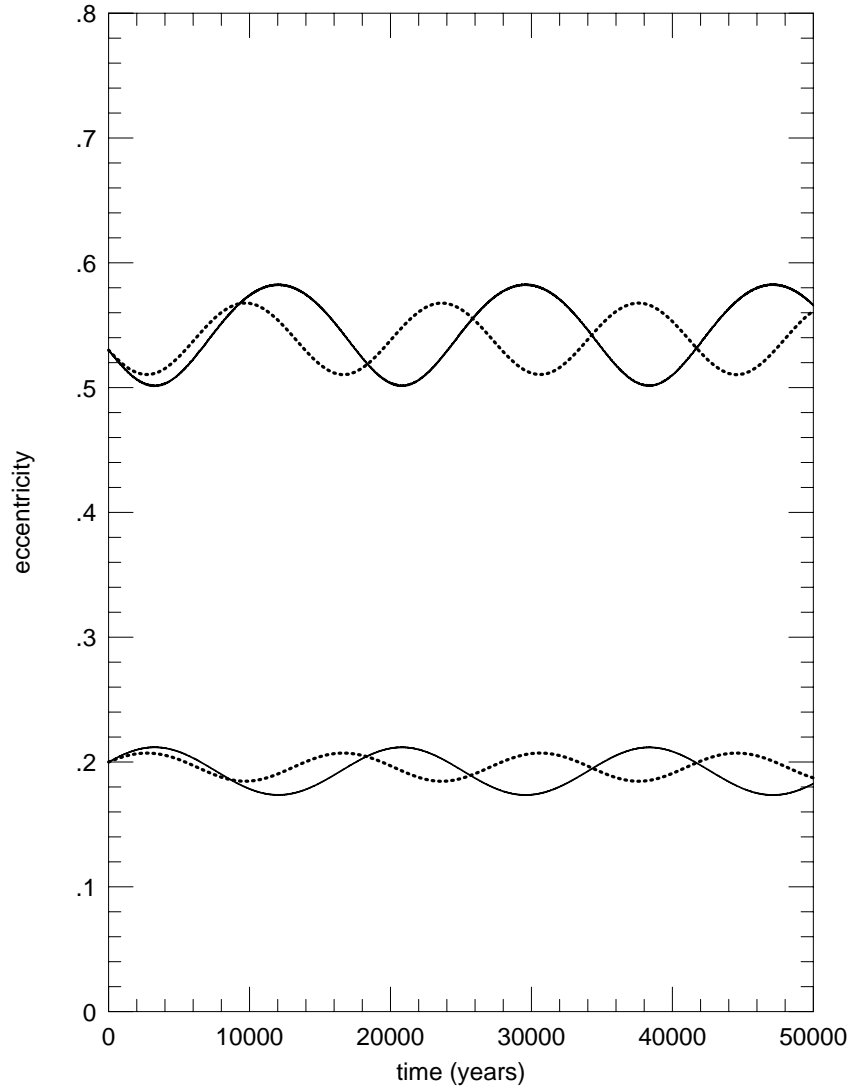


Fig. 3.— Comparison of secular theory with direct numerical integration for extrasolar planetary system HD168443. The eccentricity variations produced by direct numerical integration are shown by the solid curves; the corresponding eccentricity variations predicted by secular theory are shown by the dotted curves. The two approaches are in good agreement.



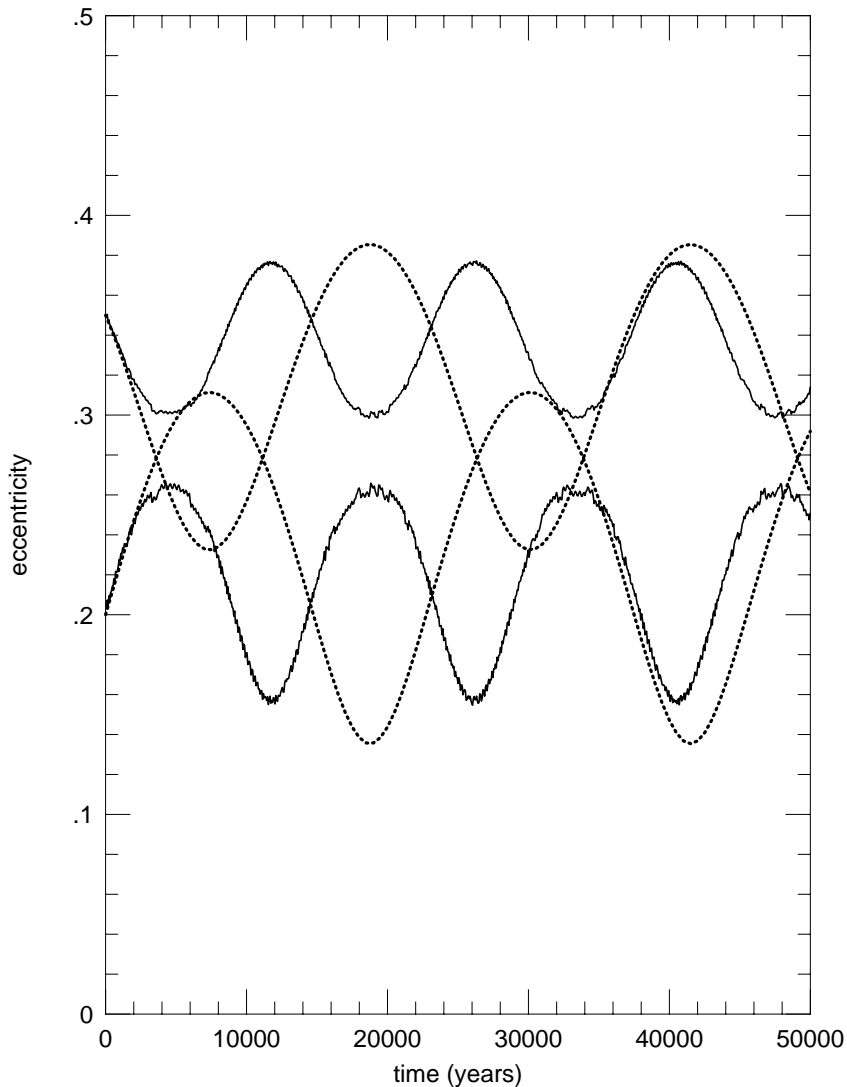


Fig. 4.— Comparison of secular theory with direct numerical integration for extrasolar planetary system HD12661. The dotted curves show the result of the secular theory discussed in the text. The two sets of solid curves show the result of direct numerical integration using two different sets of starting parameters (both within the observational uncertainties). The results show considerable variation between the two sets of starting parameters and between the numerical and secular integrations. Nonetheless, the overall envelope of eccentricity variation – and hence the distribution of eccentricities sampled by the planets – is similar for the cases shown here.

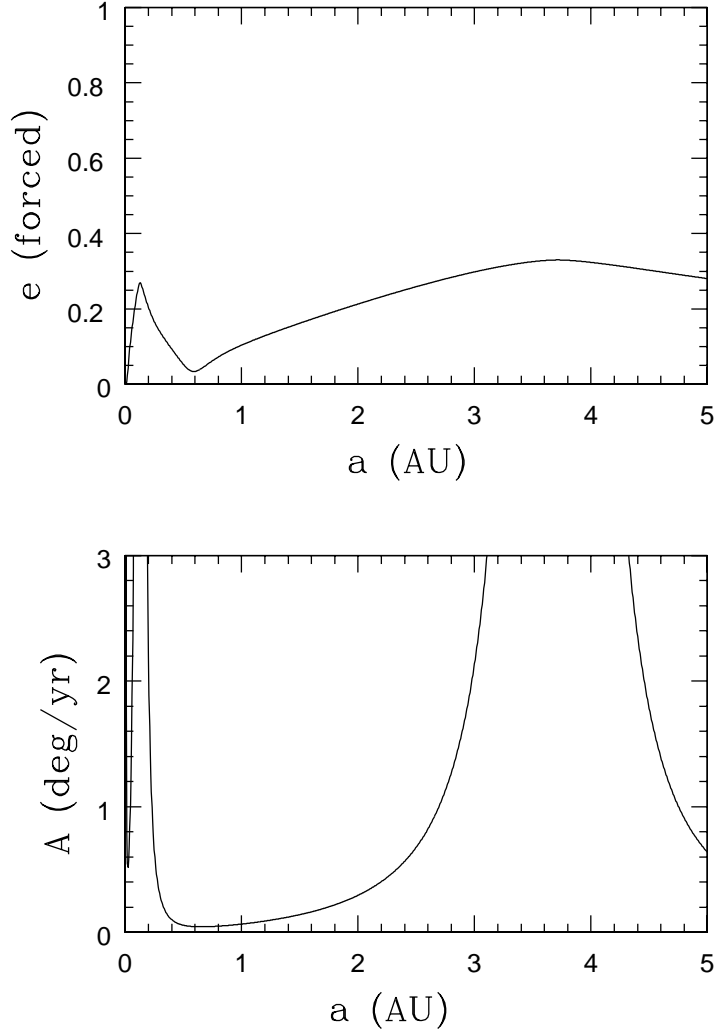


Fig. 5.— Effects of secular interactions on a hypothetical test particle in the observed planetary system HD38529. The bottom panel shows the oscillation frequency  $A$  of the test particle as a function of its semi-major axis  $a$ . The values of the eigenfrequencies  $\lambda_1, \lambda_2$  for variations in eccentricity/periastron fall well below the solid curve. The top panel shows the forced eccentricity as a function of  $a$  for time  $t = 0$ .

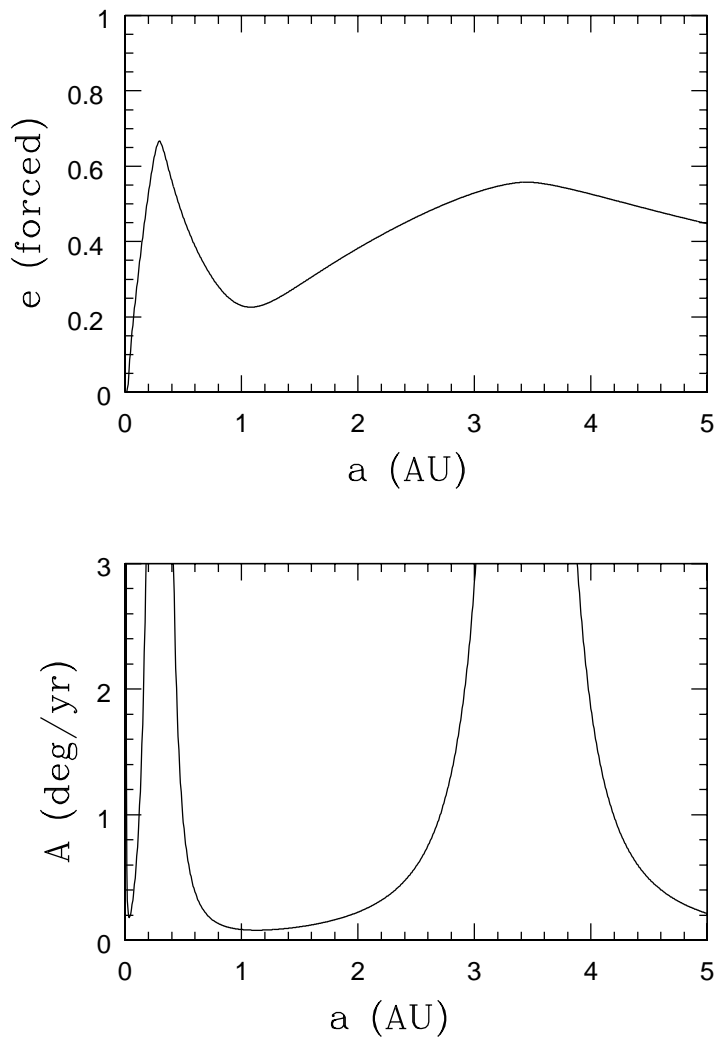


Fig. 6.— Effects of secular interactions on a hypothetical test particle in the observed planetary system HD74156. The bottom panel shows the oscillation frequency  $A$  of the test particle as a function of its semi-major axis  $a$ . The values of the eigenfrequencies  $\lambda_1, \lambda_2$  for variations in eccentricity/periastron fall well below the solid curve. The top panel shows the forced eccentricity as a function of  $a$  for time  $t = 0$ .

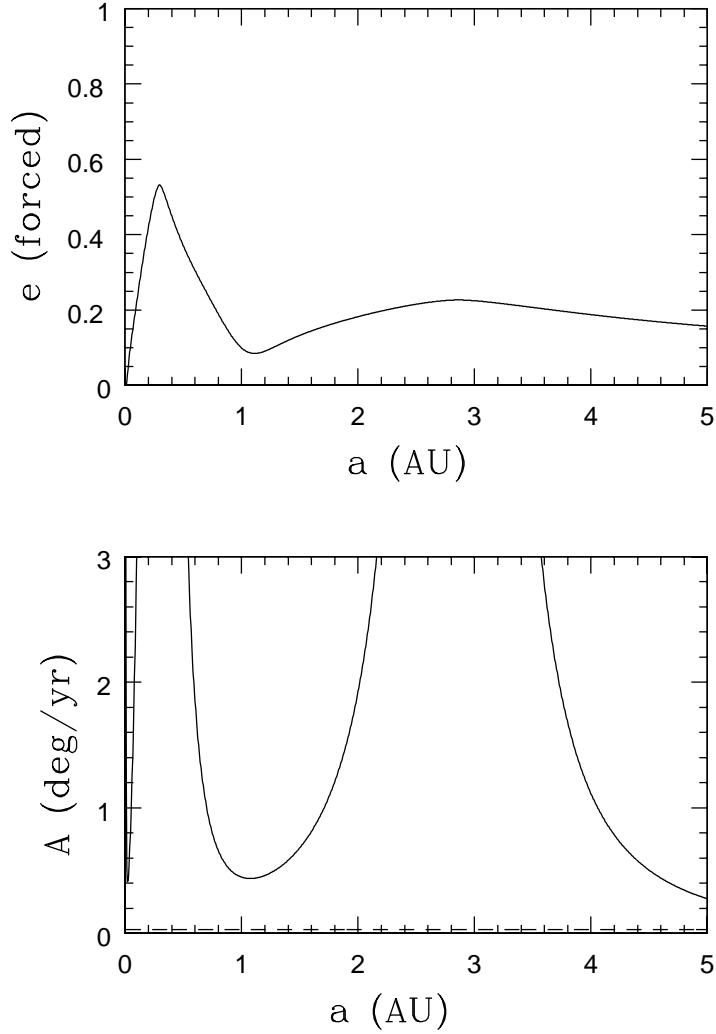


Fig. 7.— Effects of secular interactions on a hypothetical test particle in the observed planetary system HD168443. The bottom panel shows the oscillation frequency  $A$  of the test particle as a function of its semi-major axis  $a$ . The values of the eigenfrequencies  $\lambda_1, \lambda_2$  for variations in eccentricity/periastron (dashed lines) fall well below the solid curve. The top panel shows the forced eccentricity as a function of  $a$  for time  $t = 0$ .

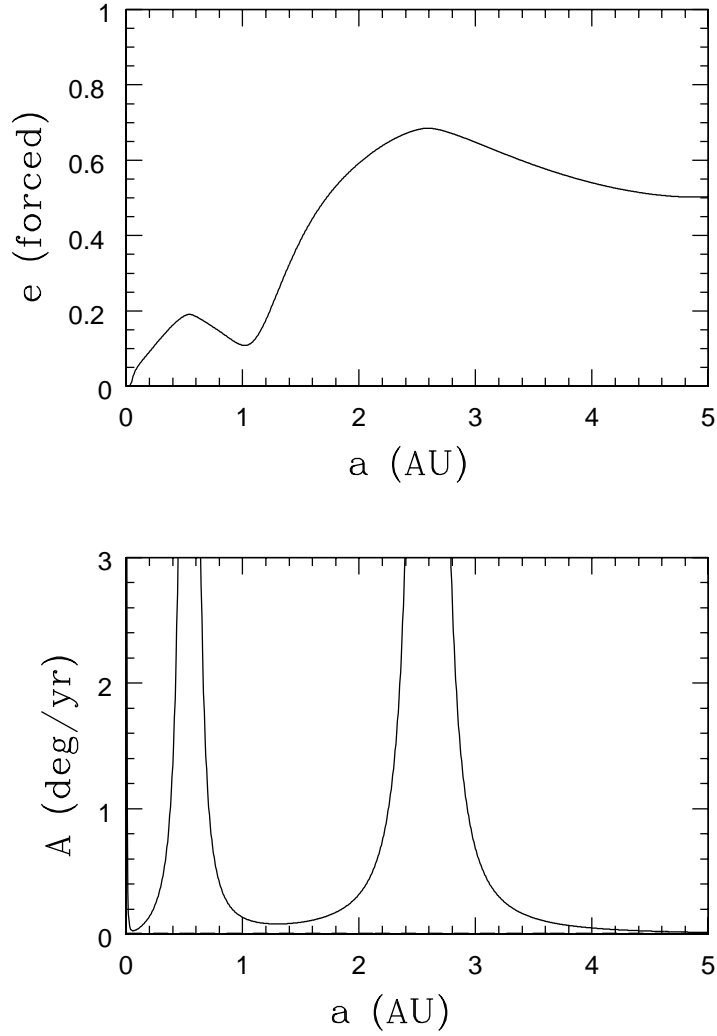


Fig. 8.— Effects of secular interactions on a hypothetical test particle in the observed planetary system HD37124. The bottom panel shows the oscillation frequency  $A$  of the test particle as a function of its semi-major axis  $a$ . The values of the eigenfrequencies  $\lambda_1, \lambda_2$  for variations in eccentricity/periastron fall well below the solid curve. The top panel shows the forced eccentricity as a function of  $a$  for time  $t = 0$ .

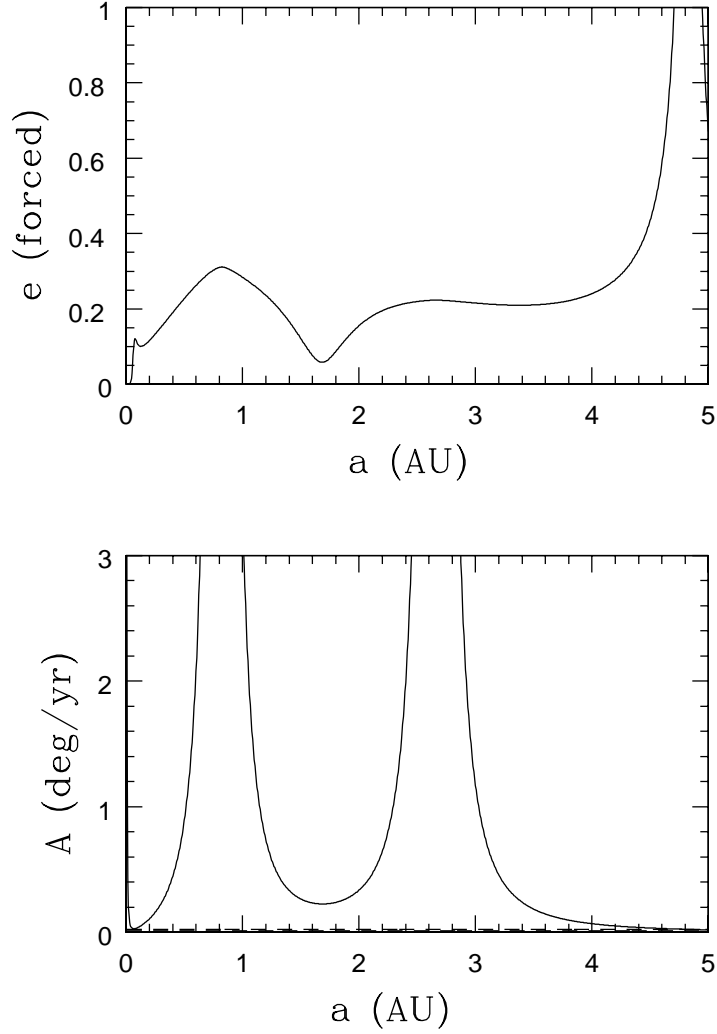


Fig. 9.— Effects of secular interactions on a hypothetical test particle in the observed planetary system HD12661. The bottom panel shows the oscillation frequency  $A$  of the test particle as a function of its semi-major axis  $a$ . The dashed horizontal lines denote the values of the eigenfrequencies  $\lambda_1, \lambda_2$  for variations in eccentricity/periastron. The top panel shows the forced eccentricity as a function of  $a$  for time  $t = 0$ .

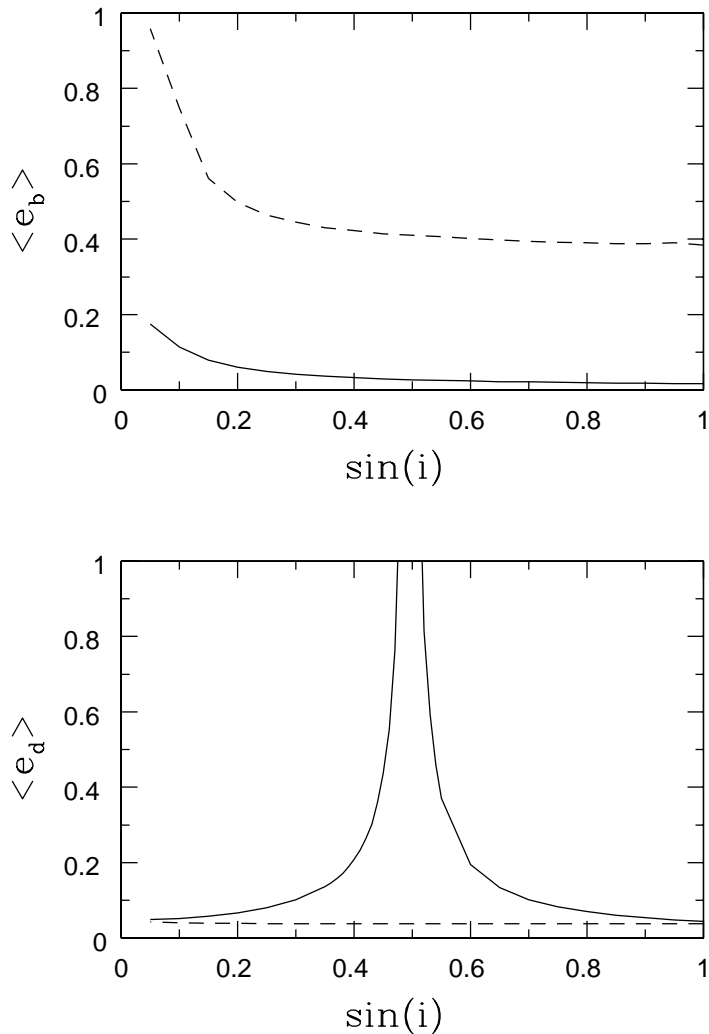


Fig. 10.— The effects of general relativistic corrections on two extrasolar planetary systems. The mean eccentricity  $\langle e \rangle$  of the innermost planet, as driven by secular interactions, is plotted as a function of  $\sin i$  for the Upsilon Andromedae system (top panel) and the HD160691 system (bottom panel). Both systems have three planets detected to date. The predictions of secular theory are shown with relativistic corrections as the solid curves, and without relativistic corrections as the dashed curves. Notice that the relativistic terms act in opposite ways in the two systems: Inclusion of relativity acts to damp eccentricity excitation by the secular interactions in the Ups And system. In the HD160691, however, they allow the system to approach a resonance for  $\sin i \approx 0.5$ .

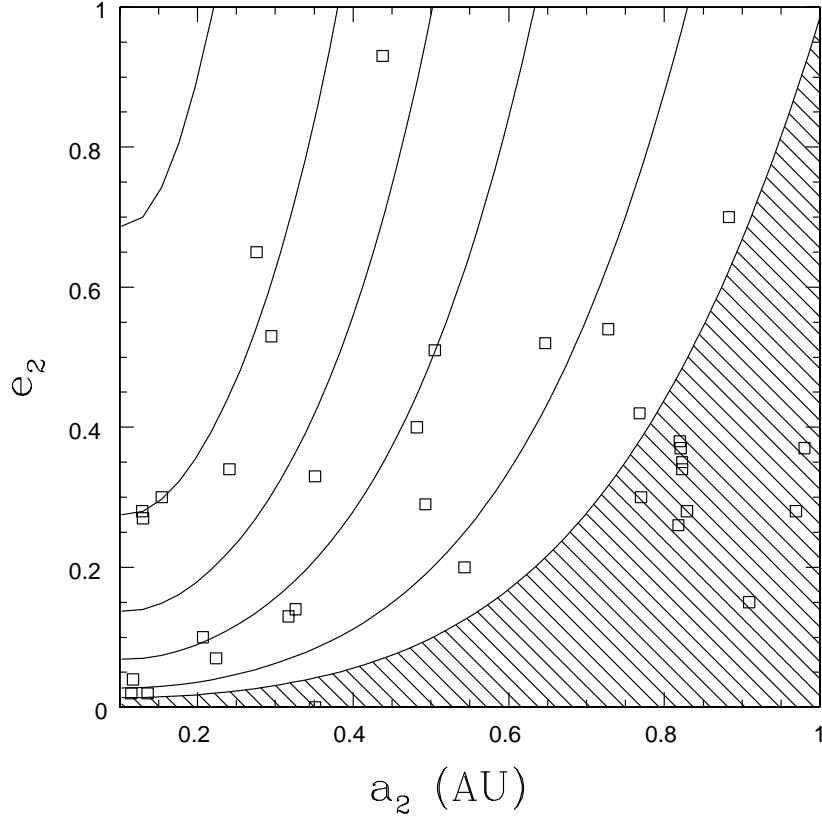


Fig. 11.— For systems that contain a hot Jupiter, a hypothetical second planet would drive the eccentricity of the inner planet to larger values. This plot shows the orbital elements of the second planet ( $a_2, e_2$ ) required to excite the eccentricity of the inner planet to given mean values. Each curve corresponds to a fixed value of the mean eccentricity of the hot Jupiter, where  $\langle e \rangle_1 = 0.01, 0.02, 0.05, 0.10, 0.20, 0.50$  (from bottom to top). The shaded region delimits the portion of the  $a - e$  plane for which additional planets have a negligible effect on the eccentricity of the hot Jupiter (where negligible is defined as  $\langle e \rangle_1 \leq 0.01$ ). For comparison, the open squares show the orbital elements of the current sample of extrasolar planets.